coatings

MDPI

Article

Preparation and Performance Study of Poly(1,3-propanediol) Ester/PLLA Blended Membrane

Dengbang Jiang [1,†], Xiushuang Song [1,†], Minna Ma [1], Huaying A [1], Jingmei Lu [1], Conglie Zi [1], Wan Zhao [1], Yaozhong Lan [2] and Mingwei Yuan [1,*]

[1] National and Local Joint Engineering Research Center for Green Preparation Technology of Biobased Materials, Yunnan Minzu University, Kunming 650500, China
[2] School of Ecology and Environmental Science, Yunnan University, Kunming 650091, China; ynulanyaozhong@163.com
* Correspondence: 041808@ymu.edu.cn
† These authors contributed equally to this work.

Abstract: Poly(1,3-propanediol palmitate)/L-polylactic acid (PO3G-PA/PLLA) composite films were prepared by solution casting. The two raw materials used to prepare the film are 100% renewable. The experimental results of the composite films show that the addition of PO3G–PA can significantly improve the toughness and crystallinity of PLLA while keeping the thermal stability of the film unchanged. When PO3G–PA was added to the film at concentrations of 0%, 5%, 10%, 15%, 20%, and 25%, the elongation at break of the film reached 37.5%, 68.8%, 118.9%, 226.8%, and 95.9%, respectively. The crystallinity of PLLA could reach 4.5%, 6.19%, 10.59%, 23.00%, 25.28%, and 16.62%, separately. The accelerated degradation experiments at 60 °C showed that adding different quantities of PO3G-PA under neutral conditions had a minimal effect on the rate of PLLA film degradation. The degradation rate of the PLLA membrane can be successfully modified by varying the concentration of PO3G–PA under acidic and alkaline conditions.

Keywords: L-polylactic acid; poly(1,3-propanediol); palmitic acid; increase resilience; film

Citation: Jiang, D.; Song, X.; Ma, M.; A, H.; Lu, J.; Zi, C.; Zhao, W.; Lan, Y.; Yuan, M. Preparation and Performance Study of Poly(1,3-propanediol) Ester/PLLA Blended Membrane. *Coatings* **2023**, *13*, 703. https://doi.org/10.3390/coatings13040703

Academic Editors: Dan Cristian Vodnar, Maria-Ioana Socaciu and Cristina Anamaria Semeniuc

Received: 22 February 2023
Revised: 25 March 2023
Accepted: 27 March 2023
Published: 30 March 2023

1. Introduction

L-polylactic acid (PLLA) is a biodegradable polyester that possesses excellent mechanical strength [1], renewability [2], and biocompatibility [3]. Films prepared by PLLA have a high potential for application in agricultural mulch film [4], food packaging film [5], and plastic bags [6], but the inherent brittleness of PLLA limits its widespread use in film applications [7,8].

Therefore, it is essential to study the toughening modification of polylactic acid films, which consists mostly of copolymerization modification and blending modification [9–11]. Copolymerization modification can preset the mechanical properties of a product by adjusting the molecular structure, although the synthesis route is complex [12–14]. Modifying the blend and composition can improve the substrate properties. The process is simple, but the compatibility of the blend directly affects the desired effect [15,16].

PLLA has been copolymerized or blended with polyethylene glycol (PEG) [17,18], poly(1,2-propanediol) (PPG) [19], polybutylene succinate (PBS) [20,21], polybutylene terephthalate (PBAT) [22], citrate [23], etc. to improve its toughness. Toncheva et al. [17] used poly(lactic acid) (PLA) and poly(ethylene glycol) (PEG) as raw materials. Antimicrobial micro- and nanofiber materials were prepared by the electrostatic spinning method. PEG was introduced by physical blending or chemical grafting. Physical blending had more significant plasticizing and toughening effects on PLA fibers. Chihaoui et al. [18] explored the feasibility of incorporating lignocellulosic nanofibers (LCNFs) into polyethylene glycol (PEG) plasticized poly(lactic acid) (PLA). The use of PEG as a carrier to produce PLA-LCNFs composites via melt processing may contribute to further highlight the merits of LCNFs

as reinforcement in a biobased polymer matrix to produce composites with enhanced mechanical properties. Xie et al. [19] investigated the effect of different molecular weights of polypropylene glycol (PPG) on the plasticizing properties of poly(lactic acid) (PLA). The lower the molecular weight of PPG, the lower the viscosity of PLA/PPG composites. The lower the mass fraction of PPG, the greater the degradation of the composites. Hu et al. [20] studied the modification of polybutadiene succinate (PBS) and polylactic acid (PLA) blends using benzoyl peroxide (BPO) as a cross-linking agent. The compatibility of PBS/PLA was improved by the addition of BPO. The addition of BPO also promoted the crystallization and complete decomposition of PBS/PLA, respectively. Moustafa et al. [22] investigated the thermal properties of poly(lactic acid) (PLA), poly(butadiene-terephthalate) adipate (PBAT), and antimicrobial natural rosin blends. The crystallization of PLA and PBAT was also investigated in detail. The cold crystallization behavior of PLA was shown. Wang S. et al. [24] prepared composites from PLLA, PEG, and multiwalled carbon nanotubes (MWCNT). The addition of PEG and the ratio of PEG to MWCNT could affect the tensile strength and elongation at the break of PLLA. Cicogna F. et al. [25] introduced different terminal functional groups on PPG. They found that the polymers formed by adipic acid had better plasticity and thermal stability.

Poly(1,3-propanediol) (PO3G) is a 100% bioderived renewable polyether polyol developed by DuPont [26,27], which has repeating units similar to PEG and PPG. Therefore, PO3G may also have a plasticizing effect on PLLA, but no studies have been reported. This work focuses on the esterification product (PO3G–PA) prepared by introducing palmitic acid (PA) onto poly(1,3-propanediol) (PO3G) through an esterification reaction. PLLA and PO3G–PA/PLLA composite films are prepared by the solution casting method. This study investigated the plasticization of low molecular weight polyester (PO3G–PA) on PLLA films.

2. Experimental

2.1. Materials

L-polylactic acid (PLLA,4032D, Nature Works, Minnetonka, MN, USA); poly(1,3-propanediol) (PO3G, Mn = 2300, DuPont, Wilmington, DE, USA); PA (Kelong Chemical Reagent Factory, Chengdu, China); 1,4-dioxane (Adamas Reagent Company, Shanghai, China); molybdenum trioxide (Adamas Reagent Company, Shanghai, China); dichloromethane: (DCM, Damao Chemical Reagent Factory, Tianjin, China).

2.2. Instrumentation

Collective thermostatic heating magnetic stirrer (DF–101S, Yuhua Instruments Co., Ltd., Gongyi, China); electrothermal blast drying oven (GZX–9240MBE, Medical Equipment Factory of Boxun Industrial Co., Ltd., Shanghai, China); electronic balance (FA2004, Koshihira Scientific Instruments Co., Ltd., Shanghai, China); 1H NMR (400 MHz Bruker Avance II, Bruker, Billerica, MA, USA); Fourier transform infrared spectrum analyzer (IS10, Nicolet, Thermo Fisher Scientific, Waltham, MA, USA); SEM (NOVA NANOSEM 450, FEI, Hillsboro, OR, USA); Microcomputer Control Universal Tensile Testing Machine (CMT4104, Chuangcheng Zhijia Technology Co., Ltd., Beijing, China); TGA (STA449F3, NETZSCH, Waldkraiburg, Germany); DSC (2414Polyma, NETZSCH, Waldkraiburg, Germany); X-ray diffractometer (D8-ADVANCE-A25X, Bruker, Billerica, MA, USA).

2.3. Sample Preparation

2.3.1. Preparation of PO3G–PA

A 250 mL three-neck flask was filled with 143.75 g of poly(1,3-propanediol) (PO3G), 32 g of PA, and 1.25 g of molybdenum trioxide. The mixture in the flask was rinsed with dry nitrogen for 15 min at room temperature. The temperature was then raised to 160 °C, and the mixture was stirred at a constant speed for 6 h under a stream of nitrogen. After heating and stirring stopped, the mixture was cooled to room temperature. An appropriate

amount of dichloromethane was added, and it was filtered by extraction and distilled under reduced pressure to produce PO3G-PA. Figure 1 shows the synthetic route for PO3G–PA.

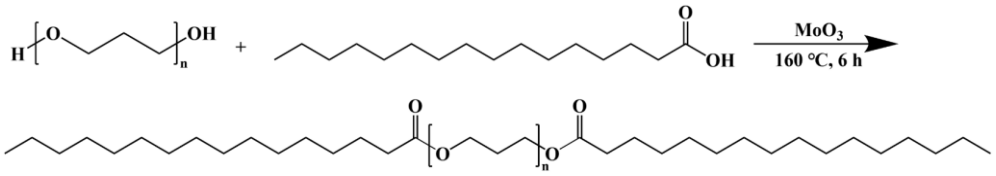

Figure 1. Synthesis route of PO3G–PA.

2.3.2. Preparation of PO3G–PA/PLLA Composite Films

A solution with a mass fraction of 20% was prepared using PLLA/PO3G-PA mixtures with PO3G content of 0%, 5%, 10%, 15%, 20%, and 25% as the solute and 1,4-dioxane as the solvent. Then, it was stirred at 65 °C until uniform. After ultrasonic debubble, the solution was applied to the clean glass with a squeegee on the 500 μm side. Composite film samples of PLLA/PO3 GPA with uniform thickness were obtained after evaporating the solvent. The samples were dried at 65 °C for 48 h, collected, and then packed for storage. The samples were labeled in the following order: pure PLLA, 5PO3G–PA/PLLA, 10PO3G–PA/PLLA, 15PO3G–PA/PLLA, 20PO3G–PA/PLLA, and 25PO3G–PA/PLLA.

2.4. Performance Testing and Structural Characterization

2.4.1. Nuclear Magnetic Resonance Test

An amount of 10 mg of PO3G and PO3G–PA was dissolved in 0.5 mL of $CDCl_3$ for testing.

2.4.2. IR Test

A Fourier transform infrared spectrometer was used to characterize the structures of PO3G–PA and PO3G–PA/PLLA composite films. The scanning range was 4000–400 cm^{-1} with 32 scans. The KBr powder was repeatedly ground and pressed, and 1 mg of the sample was dissolved in the appropriate amount of dichloromethane, coated on the KBr pressed sheet, and then tested after drying the solvent.

2.4.3. Thermal Stability Performance and Crystallization Test

The thermogravimetric analyzer explored the thermal decomposition temperature of the film samples in a nitrogen gas flow with a heating rate of 10 °C/min and a temperature range of 25 °C–600 °C. The thermal behavior of the thin film samples was analyzed by differential scanning calorimetry. Since the thermal history affects the test results of the film samples, two temperature ramps were performed at 10 °C/min with a temperature range of −40 °C–190 °C. An X-ray diffractometer was used to study the crystal structure of the thin film samples. The crystallinity X_c of PLLA in the thin film sample was obtained using Equation (1):

$$X_c = \frac{\Delta H_m - \Delta H_{CC}}{\Delta H_0 \times \omega_{PLLA}} \times 100\% \quad (1)$$

where ΔH_m is the melting enthalpy of the film sample, ΔH_{CC} is the enthalpy of cold crystallization of PLLA in the film sample, ΔH_0 is the enthalpy of crystallization when PLLA is fully crystallized under ideal conditions (93.6 J/g), and ω_{PLLA} is the mass fraction of PLLA in the film sample.

2.4.4. Mechanical Properties Testing

The film samples were tested for tensile strength and elongation at break using an electronic universal testing machine. The tensile specimens were cut into rectangles measuring 50 × 20 mm^2, the tensile rate was set to 10 mm/min, each sample was repeated five times for each test, and the average value was determined.

2.4.5. Morphological Testing

Scanning electron microscopy was used to analyze the microscopic surface morphology of the film samples. Randomly selected samples that had been dried for 12 h were cut into squares measuring 5 × 5 mm^2. To boost the electrical conductivity of samples, they were placed on a specimen table with conductive adhesive and sprayed with gold for 30 s. Images of the surface structure of the samples were then observed at different magnifications and photographed using electron microscopy.

2.4.6. Biodegradability Testing

Twenty-one square samples of each film sample measuring 20 × 20 mm^2 were prepared, dried to a constant weight in a vacuum oven at 65 °C for 20 h, and weighed, and the initial mass m_0 was recorded. The cut samples were loaded into 21 sample bottles and 20 mL of the configured buffer solution (pH = 3.0, 7.0, or 11.0 buffer solution) was added before tightening the caps. The sample vials were heated to 60 °C in an oven. The buffer was renewed every 48 h. The duration of this degradation experiment was set at 21 days. Each day, one sample was collected for drying, weighing, and calculating the rate of weight remaining rate.

3. Results and Discussion

3.1. Nuclear Magnetic Resonance Hydrogen Spectroscopy of PO3G–PA

Figure 2 shows the 1H NMR spectra of PA, PO3G, and PO3G–PA. In palmitic acid, the peak with a chemical shift of 2.3 ppm in the PA spectrum corresponds to -CH_2-(C=O)OH, the peak with a chemical shift of 1.2 ppm corresponds to -CH_2-CH_2-CH_2-, and the peak with a chemical shift of 0.75 ppm corresponds to CH_3-CH_2-. In the PO3G spectrum, the peak with a chemical shift of 3.55 ppm corresponds to -CH_2-OH, the peak with a shift of 3.4 ppm corresponds to -CH_2-CH_2-O, and the peak with a shift of 1.8 ppm corresponds to -CH_2-CH_2-CH_2-. In the plot of PO3G, the integrated areas of three peaks with chemical shifts of 3.55 ppm, 3.4 ppm, and 1.8 ppm were 1, 19.67, and 39.11, respectively. With Mn = 2300, the average degree of polymerization of PO3G was calculated to be about 20. The peaks at 3.55 ppm in the PO3G–PA spectrum showed a high chemical shift of 4.1 ppm compared with the spectrum of PO3G. The peak at 4.1 ppm is a chemical shift of -CH_2-O(C=O)-. This shows that all the hydroxyl groups in PO3G have been esterified with palmitic acid.

3.2. Infrared Spectroscopy of PO3G–PA and Composite Films

The FTIR spectra for PA, PO3G, and PO3G–PA are shown in Figure 3. In the spectral curve of PO3G and PO3G-PA, the characteristic absorption peak of the ether bond C-O is located at 1118 cm^{-1} and 1117 cm^{-1}, respectively. Methyl and methylene have characteristic absorption peaks at 2920 cm^{-1} and 2849 cm^{-1}, respectively. Observing the spectral curve of PO3G–PA, the characteristic absorption peak of the ester carbonyl group C=O appeared at 1736 cm^{-1}, which changed the carboxyl absorption peak at 1702 cm^{-1} compared with that of PA, showing that esterification occurred. Combined with the 1H NMR hydrogen spectrum, Figure 2 shows that the esterification products conform to the expected settings.

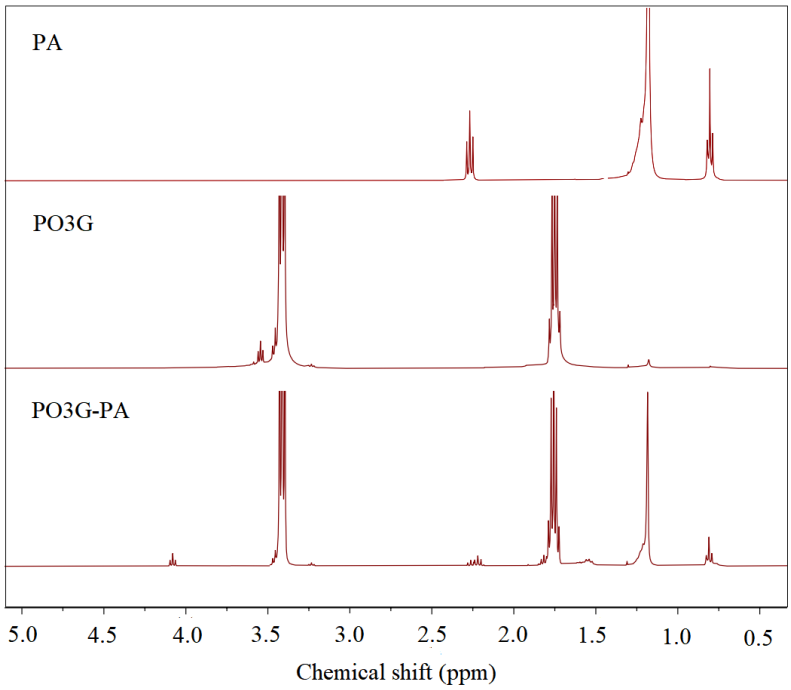

Figure 2. 1H NMR hydrogen spectra of PA, PO3G and PO3G–PA.

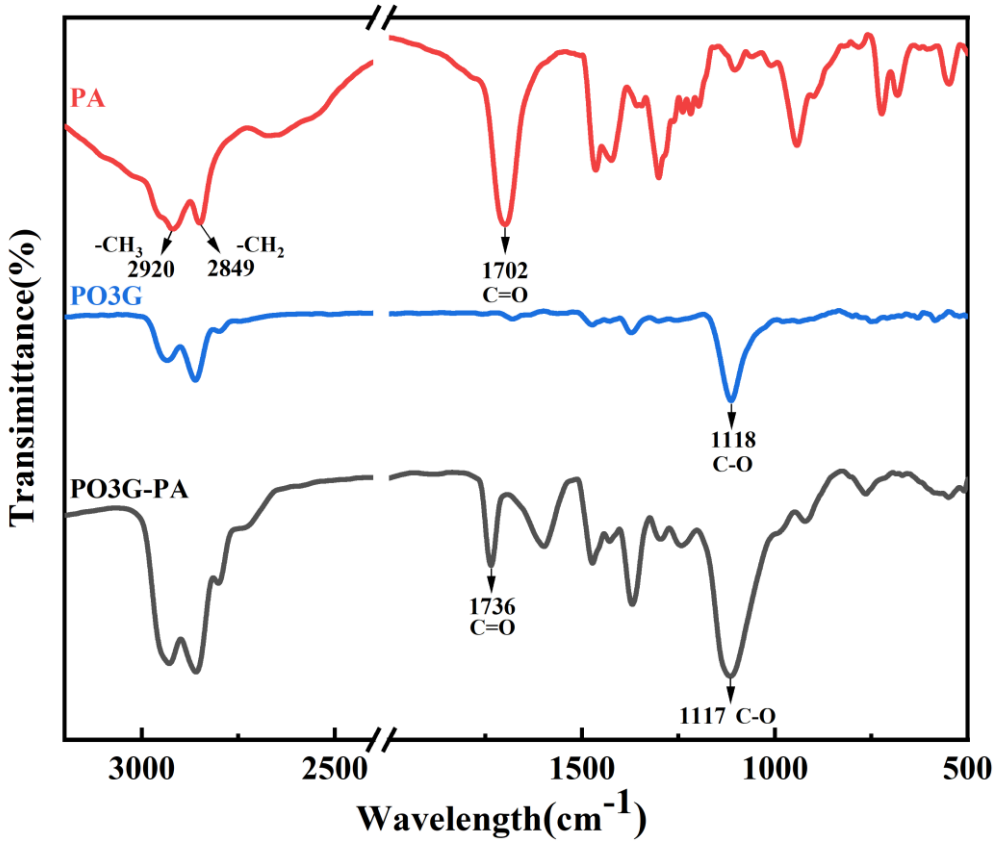

Figure 3. FTIR spectra of PA, PO3G, and PO3G–PA.

Figure 4 shows the IR spectra of PO3G–PA/PLLA composite films with different ratios. As shown in Figure 4, the positions of absorption peaks in PO3G–PA/PLLA composite films and pure PLLA are the same. The stretching vibration absorption peak of C-H in -CH3 and -CH2- is about 2900 cm^{-1}. The stretching vibration absorption peak of C=O

in PLLA and PO3G–PA is 1750 cm^{-1}. The bending vibration absorption peaks of C-H in -CH3 and -CH2- are about 1455 cm^{-1}, 1381 cm^{-1}, and 1364 cm^{-1}. The stretching vibration absorption peak of C-O lies between 1300 cm^{-1} and 1000 cm^{-1}. Comparing the IR spectra of PLLA and PO3G–PA/PLLA composite films shows neither the generation of a new characteristic absorption peak nor the disappearance of an old characteristic absorption peak, but only that the IR spectrum of the PO3G-PA/PLLA composite film was changed (peak intensity). This shows that PO3G–PA and PLLA are physically blended.

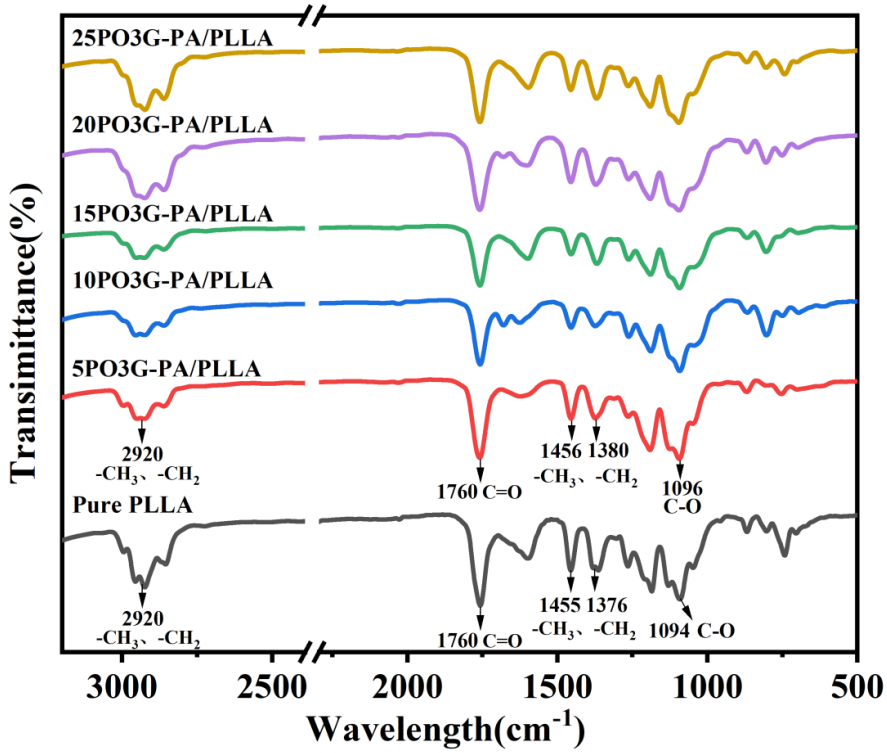

Figure 4. Infrared spectra of PO3G–PA/PLLA composite films with different ratios.

3.3. Analysis of Thermal Stability Performance and Crystallization Properties of Composite Films

Figure 5 shows the thermal weight loss (TGA) and first-order differential curve of thermal weight (DTG) for PO3G–PA/PLLA composite films with different proportions. It shows that the temperature at which the composite film loses 50% of its weight after adding different proportions of PO3G-PA is around 360 °C.

Figure 6 shows the two ramp-up curves of the DSC of PO3G–PA/PLLA composite films with different ratios. The secondary heating process eliminated distortion peaks caused by the thermal history of the sample, and the samples showed cold crystallization peaks [28]. The thermal performance parameters for the secondary heating of the sample were obtained from the curves on the right side of Figure 6. As shown in Table 1, the T_g of pure PLLA film is 60.4 °C. With increasing PO3G–PA content, the T_g of the composite films showed a decreasing trend before increasing. The lowest T_g of 20PO3G–PA/PLLA film is 49.6 °C. This shows that PO3G–PA is more compatible with PLLA when the amount of PO3G–PA added is less than 20%. The T_g begins to rise when the amount of PO3G–PA added to the composite film reaches 25%. Aggregation may occur due to the high concentration of PO3G in PLLA. The T_m of the pure PLLA film is 166.8 °C, whereas the T_m of the composite film varies little. The crystallinity of the films was 4.50%, 6.19%, 10.59%, 23.00%, 25.28%, and 16.62% when PO3G–PA was added at 0%, 5%, 10%, 15%, 20%, and 25%, respectively.

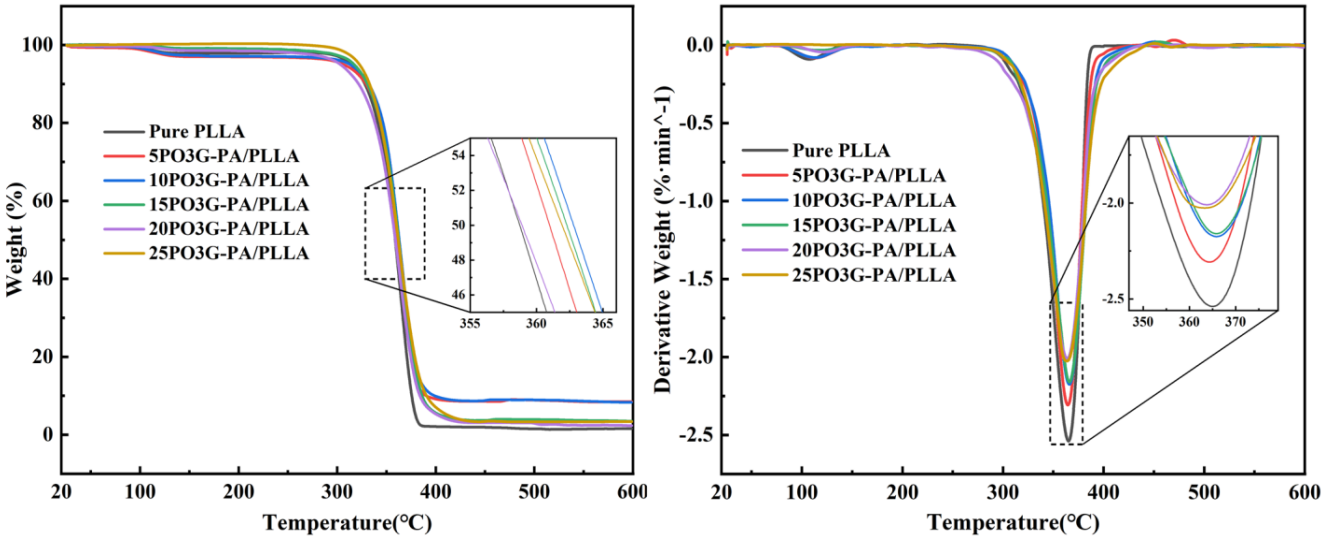

Figure 5. TG and DTG of PO3G–PA/PLLA composite films with different ratios.

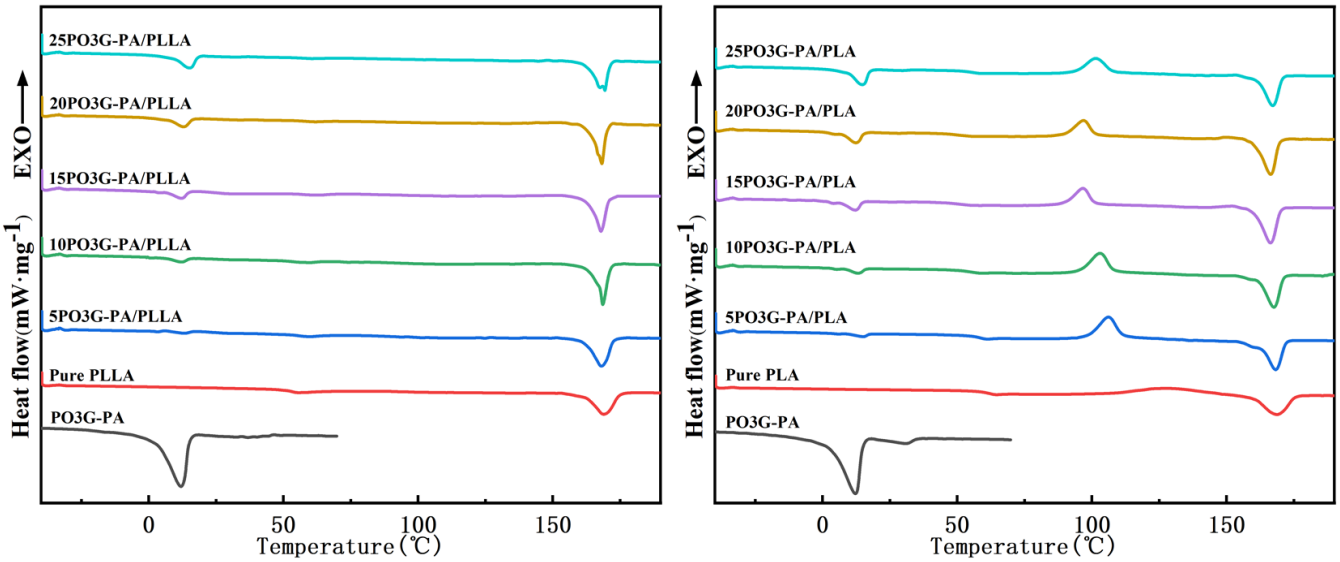

Figure 6. Primary heating and secondary heating of DSC of PO3G–PA/PLLA composite films with different ratios.

Table 1. DSC data of PO3G–PA/PLLA composite films with different ratios.

Sample	*Tg* (°C)	*Tcc* (°C)	*Tm* (°C)	ΔH_{CC} (J/g)	ΔH_m (J/g)	*Xc* (%)
Pure PLLA	60.4	129.9	166.8	25.73	33.48	4.50
5PO3G–PA/PLLA	57.3	106	168.2	27.22	32.73	6.19
10PO3G–PA/PLLA	53.6	103	167.6	24.72	33.64	10.59
15PO3G–PA/PLLA	50.1	96.7	166.3	19.5	37.8	23.00
20PO3G–PA/PLLA	49.6	96.9	166.4	18.28	37.21	25.28
25PO3G–PA/PLLA	55.1	101.5	167.1	19.45	31.21	16.62

PLLA is a polymer with a slow crystallization rate. During the film forming process of PLLA solution, the crystallization is often incomplete. Cold crystallization occurs when amorphous semi crystalline polymer systems are heated above T_g. As can be seen from Table 1, for pure PLLA, the difference between the cold crystallization enthalpy (ΔH_{CC}) and the melting enthalpy (ΔH_m) is very small, indicating that only a small amount of

crystallization occurs during the cooling process. For the "PLLA/PO3G-PA" blend, the difference between ΔH_{CC} and ΔH_m increased significantly, indicating that there was a certain degree of crystallization in these samples after the cooling process. In particular, the 20PLLA/PO3G-PA sample ΔH_m is significantly larger than ΔH_{CC}. The reason for this phenomenon is that PO3G-CA dissolved in PLLA can promote crystallization, which tends to be obvious with the increase of PO3G-CA content. Comparing the DSC curves of the two heating cycles, it can also be found that the crystallization of PLLA/PO3G-CA during the cooling process is not complete and the cold crystallization during the heating process is obvious. The phenomenon of cold crystallization depends on the ability of the chain segment to move. This indicates that after adding PO3G-CA, the chain segment motion ability of PLLA is improved. The crystallization ability of PLLA has been improved under the influence of PO3G-CA.

Figure 7 shows the XRD curves of PO3G–PA/PLLA composite films with different ratios. Furthermore, the diffraction peaks of the samples are basically in the same position, and no new diffraction peaks appeared, as shown in Figure 7. Compared with the JCPDS file (49-2174) of PLLA, the addition of PO3G–PA does not change the crystal shape of PLLA. As the amount of PO3G–PA gradually increased, the intensity of the diffraction peaks changed. As shown in Table 1, the diffraction peaks of 20PO3G–PA/PLLA were the strongest and the PLLA crystalline fraction comprised the most significant proportion. This further shows that adding a moderate amount of PO3G–PA improved the crystallinity of PLLA.

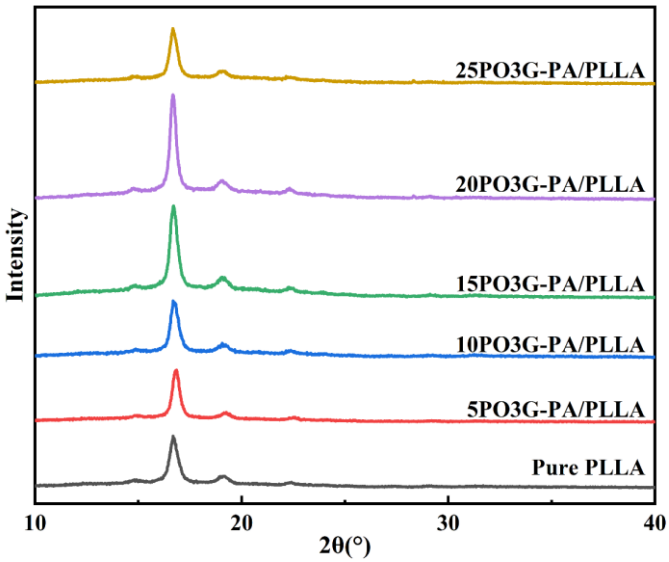

Figure 7. XRD curves of PO3G–PA/PLLA composite films with different ratios.

3.4. Analysis of Mechanical Properties of Composite Films

The modulus of elasticity measures the difficulty of producing elastic deformation of the sample, whereas elongation at break characterizes the material's soft and flexible properties. Tensile strength represents the resistance to maximum uniform plastic deformation of the material, all of which are essential factors affecting the processing and molding of the material and the performance of the finished product. Figure 8 shows the elongation at break and tensile strength of PO3G–PA/PLLA composite films with different ratios. In addition, as the amount of PO3G–PA increased, the tensile strength of the PO3G–PA/PLLA composite film gradually decreased, but the elongation at break showed a trend of first increasing before decreasing, as shown in Figure 8. Elongation at break rose from 5.7% to 226.8% when the PO3G–PA content was 0%–20%. If the PO3G–PA content increases to 25%, the elongation at break begins to decrease to 95.9%. The above phenomenon may be due to the high content of PO3G–PA, which leads to the aggregation of PO3G–PA and reduces the toughening effect on PLLA. The tensile strength of the laminated film decreased as the

PO3G–PA content increased. If the PO3G–PA content is less than 10%, the tensile strength of the composite film decreases less. If the PO3G–PA content is greater than 10%, the tensile strength of the composite film decreases more. This improved performance may be related to the molecular structure of PO3G–PA, which has ether bonds on its primary chain, allowing for easy internal rotation of PO3G–PA chain segments around the ether bonds, increasing the flexibility of the chain [29]. PO3G–PA can be used as a plasticizer for PLLA.

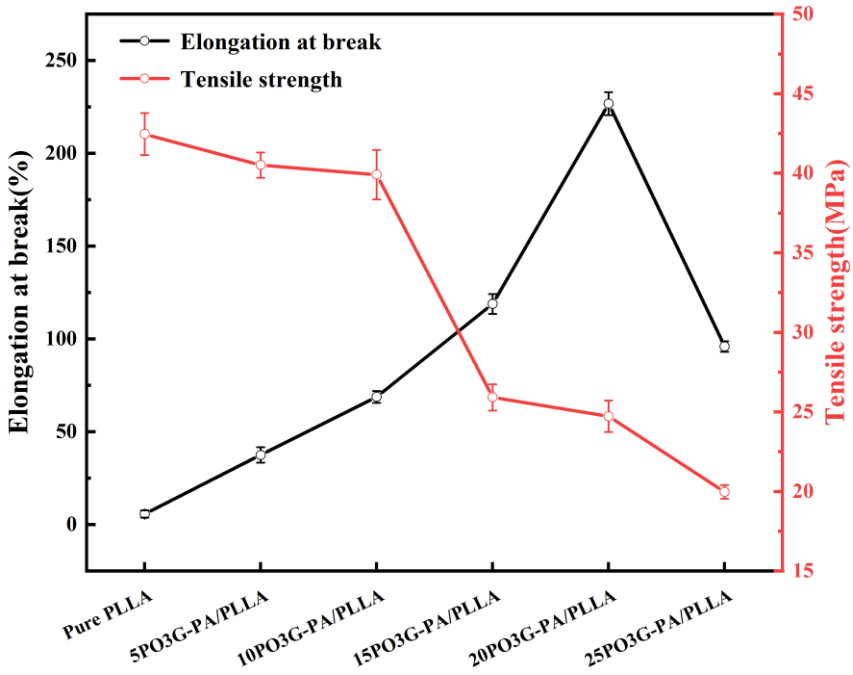

Figure 8. Elongation at break (black) and tensile strength (red) of PO3G–PA/PLLA composite films with different ratios.

3.5. Morphological Analysis of Composite Films

Figure 9 shows the photographs of PO3G–PA/PLLA composite films with different ratios. The prepared laminated film was placed on a paper sheet with "FILM" printed on it. Figure 9 shows that the macroscopic morphology of the composite film changes very little and maintains excellent transparency.

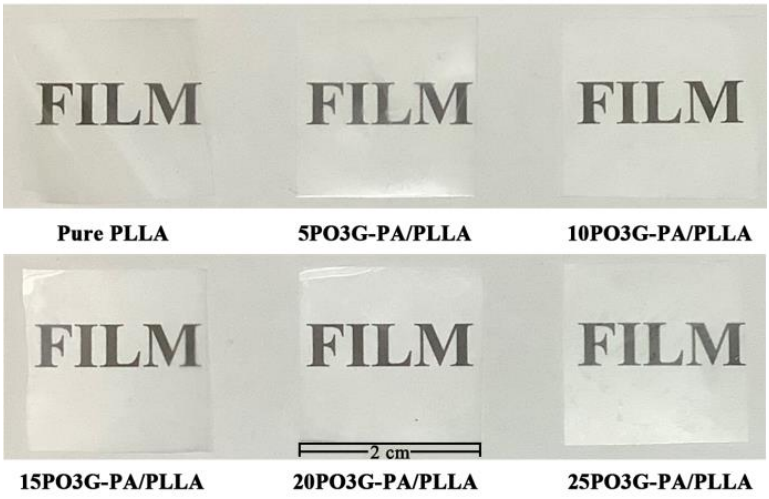

Figure 9. Surface morphology of PO3G–PA/PLLA composite films with different ratios.

Figure 10 shows the microscopic morphologies of PO3G–PA/PLLA composite films with different ratios. The surfaces of the film samples are homogeneous and relatively flat, as shown in Figure 10. As the PO3G–PA content of the film sample increases, its surfaces gradually become rough. This may be due to the slight aggregation of PO3G-PA on the film surface. The lack of significant material precipitation on surfaces shows that PLLA is compatible with PO3G–PA and that there is no significant phase separation.

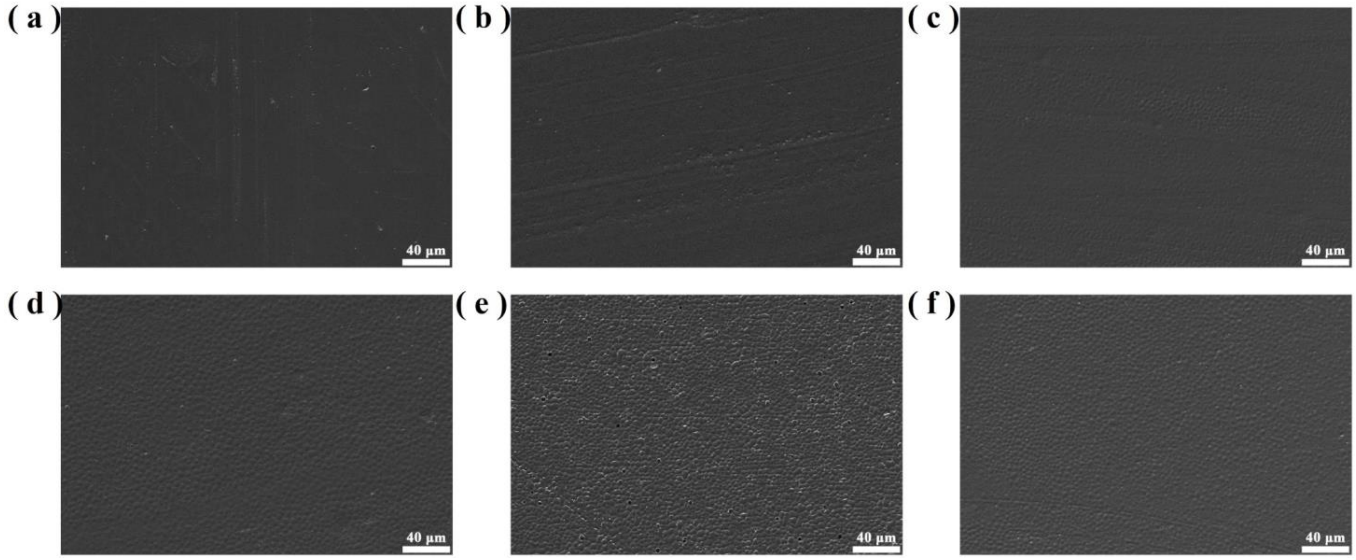

Figure 10. Microscopic morphology of PO3G–PA/PLLA composite films with different ratios. (**a**) Pure PLLA; (**b**) 5PO3G–PA/PLLA; (**c**) 10PO3G–PA/PLLA; (**d**) 15PO3G–PA/PLLA; (**e**) 20PO3G–PA/PLLA; (**f**) 25PO3G–PA/PLLA.

Figure 11 shows the tensile fracture surface morphology of PO3G–PA/PLLA composite films with different ratios. Furthermore, the section of pure PLLA film is relatively flat, a characteristic of brittle fracture, as shown in Figure 11. The cross-sections of the laminated films with different PO3G–PA content were rough and showed different degrees of tearing ligaments, a characteristic of a toughness fracture. The fracture surface of the composite film became rough with the addition of PO3G–PA, indicating that adding PO3G–PA could increase the toughness of PLLA.

Figure 11 shows that the obtained samples are porous and are characterized by a complex structure of connected pores. In order to clarify the cause of the hole formation, we have carefully observed the film surface and tensile section through SEM and found that there are no holes on all film surfaces, whereas the section containing PO3G-PA has holes. This indicates that the pores are formed due to stretching and the presence of PO3G-PA.

Due to the flexibility of PO3G-PA, it undergoes large deformation as a stress concentration point during the tensile process, overcoming the interfacial adhesion and absorbing a large amount of energy during the process of detaching from the substrate. Therefore, a large number of holes oriented along the tensile direction appear on the tensile surface. Pure PLA can produce thin necks at low strain rates, but the thin necks are still transparent and smooth without holes. Therefore, the rod-shaped holes in the tensile surface of PLLA/PO3G-PA blends are caused by the dispersed phase, which deforms the PO3G-PA along the tensile direction. The dispersed phase changes from spherical to ellipsoidal, and both ends of the ellipsoidal form energy absorption points. During the fracture process, the PLA matrix in the middle of the PO3G-PA becomes more prone to movement, resulting in shear yielding.

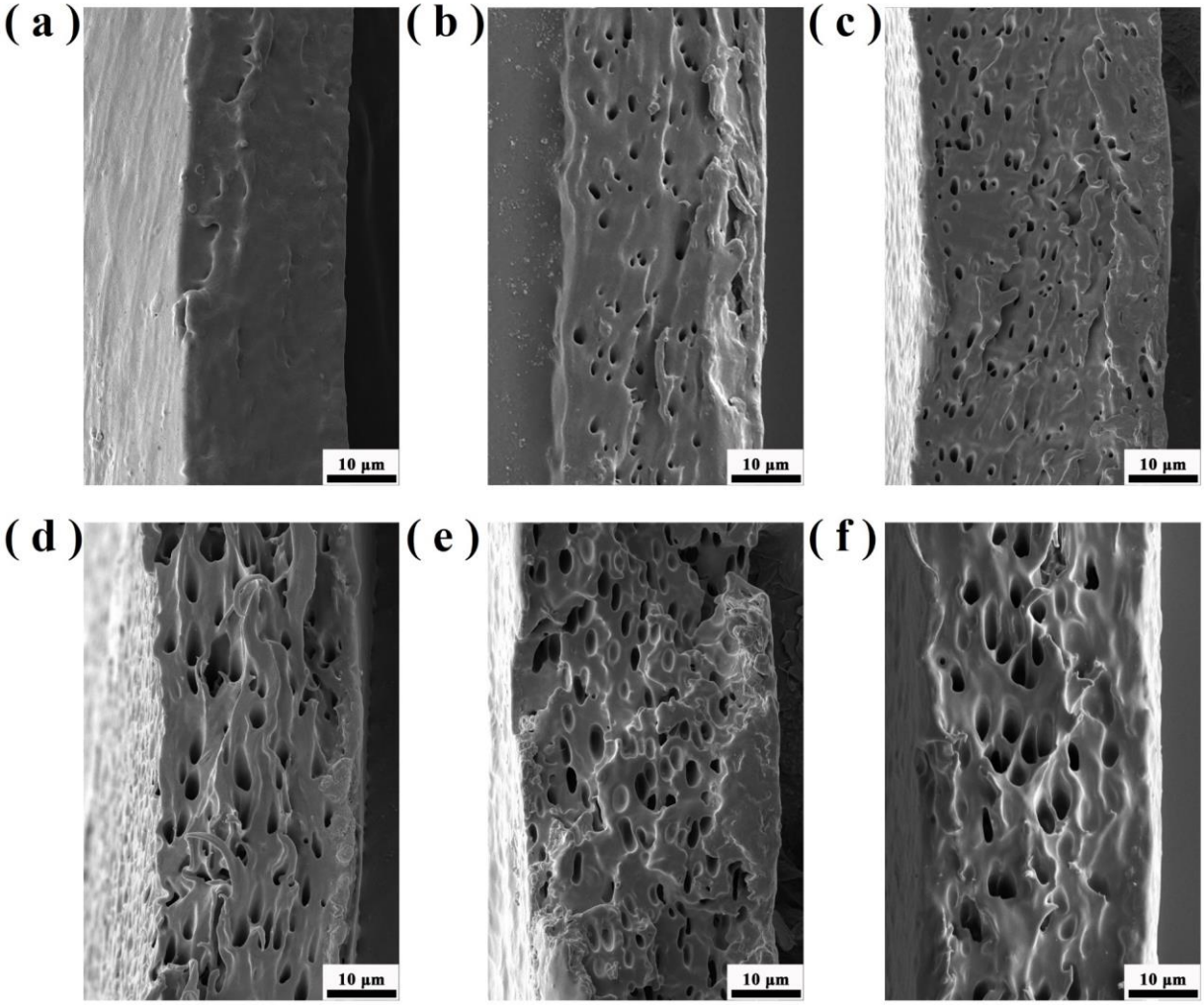

Figure 11. Tensile cross-sectional morphology of PO3G–PA/PLLA composite films at different scales. (**a**) Pure PLLA; (**b**) 5PO3G–PA/PLLA; (**c**) 10PO3G–PA/PLLA; (**d**) 15PO3G–PA/PLLA; (**e**) 20PO3G–PA/PLLA; (**f**) 25PO3G–PA/PLLA.

3.6. Analysis of Degradation Properties of Composite Films

Studies show that temperature can significantly affect the degradation rate. The degradation performance of polymer materials can be predicted by performing degradation experiments at higher temperatures to improve the experimental efficiency. A temperature near the T_g of PLLA (60 °C) was chosen to intensify the mobility of the macromolecular chains [30]. The degradation of PLLA and PO3G–PA/PLLA films is primarily the result of the hydrolysis reaction of ester bonds. The hydroxyl and carboxyl groups generated by the hydrolysis of ester bonds can increase the hydrolysis reaction, leading to the gradual degradation of the material [31,32]. The samples were rapidly degraded in acidic and alkaline conditions [33]. The degradation rate of composite films is primarily determined by two factors: first, the crystallinity of PLLA (the higher the crystallinity, the lower the degradation rate); and second, the addition of small molecule plasticizers (the higher the addition of PO3G–PA, the higher the degradation rate).

Figure 12 shows the pH degradation curves of PO3G–PA/PLLA composite films with different ratios. As shown in Figure 12b, adding PO3G–PA to composite films under neutral conditions (pH = 7) had little effect on their degradation rate. Figure 12a shows that under acidic conditions (pH = 3), a PO3G–PA content below 10% accelerates the degradation rate of the composite film. This may be due to the invasion of the small molecule plasticizer (PO3G–PA) into the chain segment of PLLA, which weakens the interaction between polymer chain segments and facilitates the attack of H+. The content of PO3G–PA above

10% decreases the degradation rate of the composite film probably because of the addition of a small molecule plasticizer (PO3G–PA), which leads to a significant increase in the crystalline properties of PLLA. As shown in Figure 12c, the degradation rate of the films in an alkaline environment (pH = 11) was faster than in acidic and neutral conditions. The degradation rate of the composite films increased as the PO3G–PA content increased.

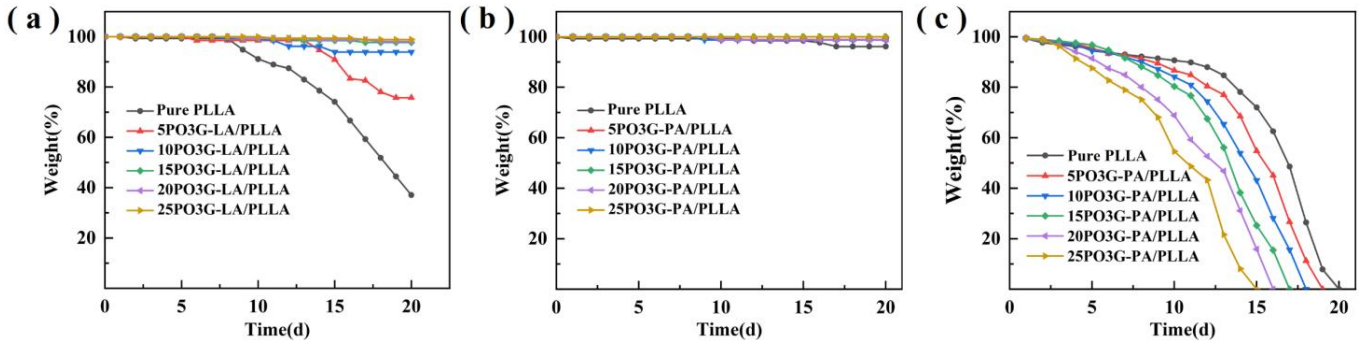

Figure 12. pH degradation curves of PO3G–PA/PLLA composite films with different ratios (**a**) pH = 3; (**b**) pH = 7; (**c**) pH = 11.

Both acids and bases can catalyze the hydrolysis of PLLA, so the degradation rate of the material under acidic and alkaline conditions is faster than under neutral conditions. Due to the faster hydrolysis rate of PO3G-PA under alkaline conditions than under acidic conditions [34,35], the presence of PO3G-PA will greatly accelerate the invasion of the solution into the interior of the film. Therefore, the degradation rate of the film under alkaline conditions is proportional to the content of PO3G-PA.

4. Conclusions

In this study, PO3G-PA was successfully prepared through polycondensation reaction. Then, using PO3G–PA as a plasticizer, PO3G–PA/PLA composite films with different PO3G–PA contents were prepared by the solution casting method. The results show that PO3G–PA and PLLA are partially compatible, and PO3G–PA can reduce the glass transition temperature and crystallization temperature of PLA, promoting the crystallization of PLLA. Adding PO3G–PA to PLLA films can effectively improve the toughness of PLLA films. When the content of PO3G–PA is 20%, the elongation at break of the PO3G–PA/PLA composite film reaches 226.8%. The degradation experiments of PO3G–PA/PLA membranes in different pH environments show that the addition of PO3G–PA can affect the degradation rate of composite membranes in acidic and alkaline environments. In alkaline environments, the degradation rate of the composite membrane is proportional to the content of PO3G–PA. In alkaline environments, when the PO3G–PA content is less than 10%, the degradation rate of PLLA films increases with the increase of PO3G content. When the content of PO3G–PA exceeds 10%, the degradation rate of the composite membrane decreases with the increase of PO3G content. The results of these studies indicate that PO3G–PA may be a suitable plasticizer for PLLA films.

Author Contributions: Conceptualization, D.J.; Methodology, D.J., H.A., J.L., C.Z., W.Z. and Y.L.; Validation, X.S.; Formal analysis, D.J. and M.M.; Investigation, D.J. and M.Y.; Resources, Y.L. and M.Y.; Data curation, X.S. and M.M.; Writing—original draft, X.S.; Writing—review & editing, D.J.; Visualization, M.M.; Project administration, D.J. and M.Y.; Funding acquisition, M.Y.. All authors have read and agreed to the published version of the manuscript.

Funding: This research was funded by National Natural Science Foundation of China (grant number: U2002215 and No.52163013), Yunnan Province "Thousand Talents Program" project training project (grant number: YNQR-CYRC-2018-012), and Yunnan Provincial Science and Technology Department (grant number: 202001AU070007).

Institutional Review Board Statement: Not applicable.

Informed Consent Statement: Not applicable.

Data Availability Statement: The data presented in this study are available on request from the corresponding author.

Conflicts of Interest: The authors declare no conflict of interest.

References

1. Barkhad, M.S.; Abu-Jdayil, B.; Mourad, A.H.I.; Iqbal, M.Z. Thermal Insulation and Mechanical Properties of Polylactic Acid (PLA) at Different Processing Conditions. *Polymers* **2020**, *12*, 2091. [CrossRef] [PubMed]
2. Rajeshkumar, G.; Arvindh Seshadri, S.; Devnani, G.L.; Sanjay, M.R.; Siengchin, S.; Prakash Maran, J.; Al-Dhabi, N.A.; Karuppiah, P.; Mariadhas, V.A.; Sivarajasekar, N.; et al. Environment friendly, renewable and sustainable poly lactic acid (PLA) based natural fiber reinforced composites—A comprehensive review. *J. Clean. Prod.* **2021**, *310*, 127483. [CrossRef]
3. Ramot, Y.; Haim-Zada, M.; Domb, A.J.; Nyska, A. Biocompatibility and safety of PLA and its copolymers. *Adv. Drug Deliv. Rev.* **2016**, *107*, 153–162. [CrossRef]
4. Merino, D.; Zych, A.; Athanassiou, A. Biodegradable and Biobased Mulch Films: Highly Stretchable PLA Composites with Different Industrial Vegetable Waste. *ACS Appl. Mater. Interfaces* **2022**, *14*, 46920–46931. [CrossRef] [PubMed]
5. Roy, S.; Rhim, J.-W. Preparation of bioactive functional poly(lactic acid)/curcumin composite film for food packaging application. *Int. J. Biol. Macromol.* **2020**, *162*, 1780–1789. [CrossRef] [PubMed]
6. Chang, Q.; Zhu, D.; Hu, L.; Kim, H.; Liu, Y.; Cai, L. Rapid photo aging of commercial conventional and biodegradable plastic bags. *Sci. Total Environ.* **2022**, *822*, 153235. [CrossRef]
7. Xuzhen, Z.; Xin, W.; Chenmeng, Z.; Wenjian, H.; Yong, L. Defects in polylactide spherulites: Ring line cracks and micropores. *Polym. Degrad. Stab.* **2021**, *183*, 109416. [CrossRef]
8. Graupner, N.; Ziegmann, G.; Müssig, J. Composite models for compression moulded long regenerated cellulose fibre-reinforced brittle polylactide (PLA). *Compos. Sci. Technol.* **2017**, *149*, 55–63. [CrossRef]
9. Yang, Y.; Zhang, L.; Xiong, Z.; Tang, Z.; Zhang, R.; Zhu, J. Research progress in the heat resistance, toughening and filling modification of PLA. *Sci. China Chem.* **2016**, *59*, 1355–1368. [CrossRef]
10. Ding, Y.; Lu, B.; Wang, P.; Wang, G.; Ji, J. PLA-PBAT-PLA tri-block copolymers: Effective compatibilizers for promotion of the mechanical and rheological properties of PLA/PBAT blends. *Polym. Degrad. Stab.* **2018**, *147*, 41–48. [CrossRef]
11. Akindoyo, J.O.; Beg, M.D.H.; Ghazali, S.; Heim, H.P.; Feldmann, M. Impact modified PLA-hydroxyapatite composites—Thermo-mechanical properties. *Compos. Part A Appl. Sci. Manuf.* **2018**, *107*, 326–333. [CrossRef]
12. Puthumana, M.; Santhana Gopala Krishnan, P.; Nayak, S.K. Chemical modifications of PLA through copolymerization. *Int. J. Polym. Anal. Charact.* **2020**, *25*, 634–648. [CrossRef]
13. Maharana, T.; Pattanaik, S.; Routaray, A.; Nath, N.; Sutar, A.K. Synthesis and characterization of poly(lactic acid) based graft copolymers. *React. Funct. Polym.* **2015**, *93*, 47–67. [CrossRef]
14. Saulnier, B.; Ponsart, S.; Coudane, J.; Garreau, H.; Vert, M. Lactic Acid-Based Functionalized Polymers via Copolymerization and Chemical Modification. *Macromol. Biosci.* **2004**, *4*, 232–237. [CrossRef]
15. Lyu, Y.; Pang, J.; Gao, Z.; Zhang, Q.; Shi, X. Characterization of the compatibility of PVC/PLA blends by Aid of Rheological Responses. *Polymer* **2019**, *176*, 20–29. [CrossRef]
16. Nagarajan, V.; Mohanty, A.K.; Misra, M. Perspective on Polylactic Acid (PLA) based Sustainable Materials for Durable Applications: Focus on Toughness and Heat Resistance. *ACS Sustain. Chem. Eng.* **2016**, *4*, 2899–2916. [CrossRef]
17. Toncheva, A.; Mincheva, R.; Kancheva, M.; Manolova, N.; Rashkov, I.; Dubois, P.; Markova, N. Antibacterial PLA/PEG electrospun fibers: Comparative study between grafting and blending PEG. *Eur. Polym. J.* **2016**, *75*, 223–233. [CrossRef]
18. Chihaoui, B.; Tarrés, Q.; Delgado-Aguilar, M.; Mutjé, P.; Boufi, S. Lignin-containing cellulose fibrils as reinforcement of plasticized PLA biocomposites produced by melt processing using PEG as a carrier. *Ind. Crops Prod.* **2022**, *175*, 114287. [CrossRef]
19. Xie, D.; Zhao, Y.; Li, Y.; LaChance, A.M.; Lai, J.; Sun, L.; Chen, J. Rheological, Thermal, and Degradation Properties of PLA/PPG Blends. *Materials* **2019**, *12*, 3519. [CrossRef]
20. Hu, X.; Su, T.; Li, P.; Wang, Z. Blending modification of PBS/PLA and its enzymatic degradation. *Polym. Bull.* **2018**, *75*, 533–546. [CrossRef]
21. Su, S.; Kopitzky, R.; Tolga, S.; Kabasci, S. Polylactide (PLA) and Its Blends with Poly(butylene succinate) (PBS): A Brief Review. *Polymers* **2019**, *11*, 1193. [CrossRef]
22. Moustafa, H.; El Kissi, N.; Abou-Kandil, A.I.; Abdel-Aziz, M.S.; Dufresne, A. PLA/PBAT Bionanocomposites with Antimicrobial Natural Rosin for Green Packaging. *ACS Appl. Mater. Interfaces* **2017**, *9*, 20132–20141. [CrossRef]
23. Stoll, L.; Domenek, S.; Hickmann Flôres, S.; Nachtigall, S.M.B.; Oliveira Rios, A. Polylactide films produced with bixin and acetyl tributyl citrate: Functional properties for active packaging. *J. Appl. Polym. Sci.* **2021**, *138*, 50302. [CrossRef]
24. Wang, S.; Wu, R.; Zhang, J.; Leng, Y.; Li, Q. PLA/PEG/MWCNT composites with improved processability and mechanical properties. *Polym. Plast. Technol. Mater.* **2021**, *60*, 430–439. [CrossRef]
25. Cicogna, F.; Coiai, S.; De Monte, C.; Spiniello, R.; Fiori, S.; Franceschi, M.; Braca, F.; Cinelli, P.; Fehri, S.M.K.; Lazzeri, A.; et al. Poly(lactic acid) plasticized with low-molecular-weight polyesters: Structural, thermal and biodegradability features: PLA plasticized with low-molecular-weight polyesters. *Polym. Int.* **2017**, *66*, 761–769. [CrossRef]

26. Vo, A.D.; Cui, W.J.; McAuley, K.B. An Improved PO3G Model–Accounting for Cyclic Oligomers. *Macromol. Theory Simul.* **2020**, *29*, 2000023. [CrossRef]
27. Zhang, C.; Luan, H.; Wang, G. A novel thermosensitive triblock copolymer from 100% renewably sourced poly(trimethylene ether) glycol. *J. Appl. Polym. Sci.* **2018**, *135*, 46112. [CrossRef]
28. Zhu, Z.; Li, W.; Yin, Y.; Cao, R.; Li, Z. Differential Scanning Calorimetry Material Studies: Benzil Melting Point Method for Eliminating the Thermal History of DSC. *J. Chem.* **2022**, *1*, 3423429. [CrossRef]
29. Yang, J.-X.; Qian, H.-J.; Gong, Z.; Lu, Z.-Y.; Cui, S.-X. Stretching Elasticity and Flexibility of Single Polyformaldehyde Chain. *Chin. J. Polym. Sci.* **2022**, *40*, 333–337. [CrossRef]
30. Rodriguez, E.J.; Marcos, B.; Huneault, M.A. Hydrolysis of polylactide in aqueous media. *J. Appl. Polym. Sci.* **2016**, *133*, 35–42. [CrossRef]
31. Simmons, H.; Kontopoulou, M. Hydrolytic degradation of branched PLA produced by reactive extrusion. *Polym. Degrad. Stab.* **2018**, *158*, 228–237. [CrossRef]
32. Momeni, S.; Rezvani Ghomi, E.; Shakiba, M.; Shafiei-Navid, S.; Abdouss, M.; Bigham, A.; Khosravi, F.; Ahmadi, Z.; Faraji, M.; Abdouss, H.; et al. The Effect of Poly(Ethylene glycol) Emulation on the Degradation of PLA/Starch Composites. *Polymers* **2021**, *13*, 1019. [CrossRef]
33. Elsawy, M.A.; Kim, K.-H.; Park, J.-W.; Deep, A. Hydrolytic degradation of polylactic acid (PLA) and its composites. *Renew. Sustain. Energy Rev.* **2017**, *79*, 1346–1352. [CrossRef]
34. Tsuji, H.; Ikada, Y. Properties and morphology of poly(l-lactide) 4. Effects of structural parameters on long-term hydrolysis of poly(l-lactide) in phosphate-buffered solution. *Polym. Degrad. Stab.* **2000**, *67*, 179–189. [CrossRef]
35. Tsuji, H.; Ikarashi, K. In vitro hydrolysis of poly(l-lactide) crystalline residues as extended-chain crystallites: III. Effects of pH and enzyme. *Polym. Degrad. Stab.* **2004**, *85*, 647–656. [CrossRef]